Pergamon

Geochimica et Cosmochimica Acta, Vol. 65, No. 22, pp. 4243–4255, 2001

0016-7037/01 $20.00 + .00

PII S0016-7037(01)00687-1

Sr-Nd-Pb isotope systematics of mantle xenoliths from Somerset Island kimberlites: Evidence for lithosphere stratification beneath Arctic Canada

S. S. SCHMIDBERGER,[1,*] A. SIMONETTI,[2] and D. FRANCIS[1]

[1]Earth and Planetary Sciences, McGill University, 3450 University Street, Montréal, Québec, H3A 2A7, Canada
[2]GEOTOP, Université du Québec à Montréal, CP 8888 succ. Centreville, Montréal, Québec, H3C 3P8, Canada

(*Received December* 14, 2000; *accepted in revised form May* 17, 2001)

Abstract—Sr, Nd, and Pb isotopic compositions were determined for a suite of Archean garnet peridotite and garnet pyroxenite xenoliths and their host Nikos kimberlite (100 Ma) from Somerset Island to constrain the isotopic character of the mantle root beneath the northern Canadian craton. The Nikos peridotites are enriched in highly incompatible trace elements ($La/Sm_N = 4–6$), and show $^{143}Nd/^{144}Nd_{(t)}$ (0.51249–0.51276) and a large range in $^{87}Sr/^{86}Sr_{(t)}$ (0.7047–0.7085) and Pb ($^{206}Pb/^{204}Pb_{(t)}$ = 17.18 to 19.03) isotope ratios that are distinct from those estimated for "depleted mantle" compositions at the time of kimberlite emplacement. The Nd isotopic compositions of the peridotites overlap those of the Nikos kimberlite, suggesting that the xenoliths were contaminated with kimberlite or a kimberlite-related accessory phase (i.e., apatite). The highly variable Sr and Pb isotopic compositions of the peridotites, however, indicate that kimberlite contribution was restricted to very small amounts (~1 wt % or less).

The high-temperature peridotites (>1100°C) that sample the deep Somerset lithosphere trend toward more radiogenic $^{87}Sr/^{86}Sr_{(t)}$ (0.7085) and unradiogenic $^{206}Pb/^{204}Pb_{(t)}$ (17.18) isotopic ratios than those of the low-temperature peridotites (<1100°C). This is in agreement with Sr isotopic compositions of clinopyroxene from the low-temperature peridotites ($^{87}Sr/^{86}Sr_{(t)} = 0.7038–0.7046$) that are significantly less radiogenic than those of clinopyroxene from the high-temperature peridotites ($^{87}Sr/^{86}Sr_{(t)} = 0.7052–0.7091$). The depth correlation of Sr isotopes for clinopyroxene and Sr and Pb isotopic compositions for the Nikos whole-rocks indicate that the deep Somerset lithosphere (>160 km) is isotopically distinct from the shallow lithospheric mantle. The isotopic stratification with depth suggests that the lower lithosphere is probably younger and may have been added to the existing Archean shallow mantle in a Phanerozoic magmatic event. The radiogenic Sr isotope ratios of the high-temperature peridotites and their clinopyroxenes suggest that the underplated deep lithosphere contained recycled (altered oceanic crust and sedimentary component?) material introduced during earlier subduction. *Copyright © 2001 Elsevier Science Ltd*

1. INTRODUCTION

Archean cratons are underlain by cold refractory mantle roots characterized by a depletion in fusible major elements compared with fertile mantle (e.g., Nixon, 1987; Herzberg, 1993; McDonough, 1990; Boyd et al., 1997). In contrast to their refractory major element chemistry, however, the peridotites that sample these mantle roots are frequently trace-element enriched, suggesting that the lithosphere may constitute a significant reservoir for incompatible elements (Erlank et al., 1987; Menzies et al., 1987). Mantle xenoliths that are brought to the surface by kimberlites and alkali basalts are a unique window into the subcontinental mantle and provide essential insights into the isotopic character and evolution of the lithosphere to depths of greater than 200 km. Previous studies have shown that these peridotite xenoliths have a large range in Sr, Nd, and Pb isotopic compositions and trend toward "enriched" time-integrated isotopic signatures relative to bulk Earth (e.g., Menzies and Murthy, 1980; Hawkesworth et al., 1990a; Pearson et al., 1995a). This is inconsistent with their origin as residues of partial melting, which should create refractory mantle roots with an isotopic signature similar to that of "depleted mantle" (Zindler and Hart, 1986). Such isotopic heterogeneities have been widely interpreted to indicate that the subcontinental lithosphere has been infiltrated by small volume melts or fluids with highly variable isotopic compositions over time. These melts or fluids were enriched in large ion lithophile elements (LILE) and light rare earth elements (LREE) and originated from deeper levels of the lithosphere or from the underlying asthenosphere (Erlank et al., 1987; Menzies et al., 1987). Thus, the isotopic systematics of samples representing the subcratonic mantle are sensitive indicators of the metasomatic history they have experienced and provide evidence for the existence of isotopically distinct domains in the lithosphere and a means to constrain their spatial distribution.

In this article, we present Sr, Nd, and Pb isotopic compositions for a suite of garnet peridotites and garnet pyroxenites and their host Nikos kimberlite from Somerset Island in the Canadian Arctic (Schmidberger and Francis, 1999; Fig. 1). The results for whole-rocks and constituent mineral phases (i.e., clinopyroxene, garnet) provide insights into the isotopic signature of the deep Archean mantle root beneath the northern Canadian craton. The data set indicates a change in isotopic composition with depth in the lithospheric mantle and provides constraints on the role of the host kimberlite as a possible contaminant during sample transport.

2. SAMPLES

2.1. Kimberlite

The recently discovered Nikos kimberlites were emplaced into late Archean crystalline basement overlain by Paleozoic

* Author to whom correspondence should be addressed (stefanie@eps.mcgill.ca).

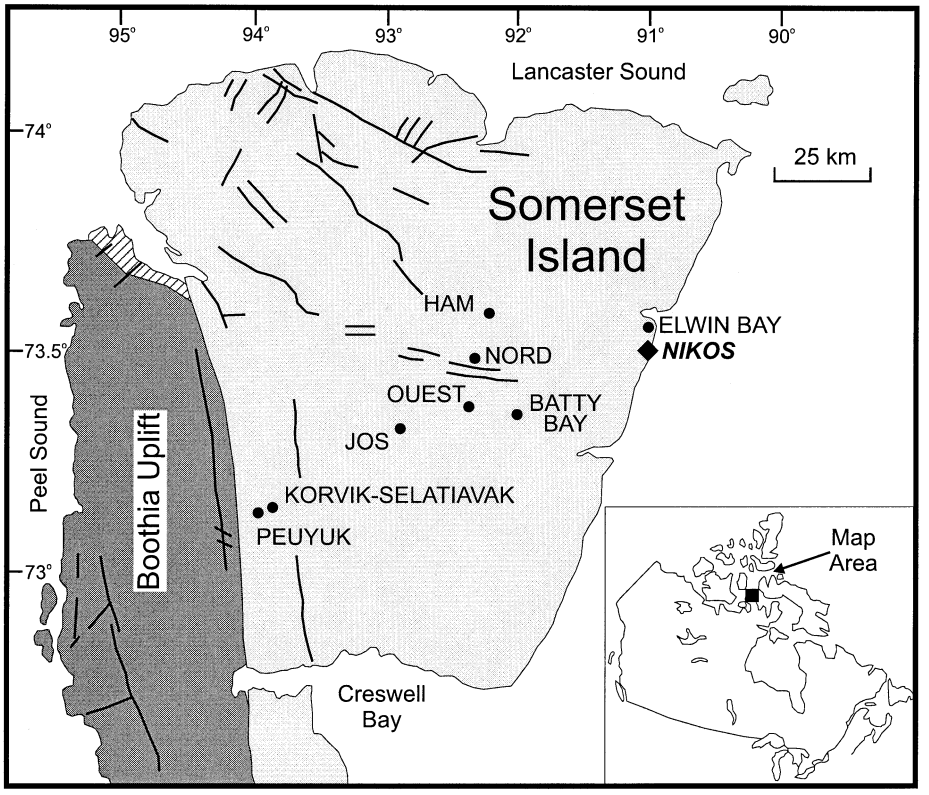

Fig. 1. Geological map of Somerset Island (after Steward; 1987) showing kimberlite locations. The mantle xenoliths from this study were collected from the Nikos kimberlite pipes (black diamond). Legend: light gray, Paleozoic cover rocks; striped, Late Proterozoic cover rocks; dark gray, Precambrian basement; bold lines, normal faults.

sediments at the northern margin of the Canadian craton (Frisch and Hunt, 1993; Pell, 1993; Fig. 1). U-Pb dating of perovskite indicates Cretaceous emplacement ages between 90 to 105 Ma for the Somerset Island kimberlites (Heaman, 1989; Smith et al., 1989). An Rb-Sr whole-rock isochron for the Nikos kimberlites (n = 4) from this study yields an emplacement age of 97 ± 17 Ma (MSWD = 1.1), which is in good agreement with the U-Pb ages.

The southernmost of the three individual Nikos pipes (NK3) has been interpreted to represent kimberlite magma (Schmidberger and Francis, 1999) because of the nonclastic microcrystalline nature of its groundmass. The kimberlite contains olivine, phlogopite, garnet, and spinel in a very fine-grained, carbonate-rich matrix of calcite, serpentine, perovskite, and apatite. The very high $CaCO_3$ contents (27–39 wt. %; Schmidberger and Francis, 1999) of the kimberlite whole-rock analyses indicate liquid compositions intermediate between kimberlite and carbonatite (Woolley and Kempe, 1989; Ringwood et al., 1992). The kimberlites show a strong enrichment in highly incompatible trace elements, such as LILE and LREE, compared with primitive mantle compositions and chondrites (McDonough and Sun, 1995; Schmidberger and Francis, 2001).

2.2. Mantle Xenoliths

The Nikos xenolith suite consists of large (>10 cm), well-preserved garnet peridotites with minor occurrences of garnet pyroxenites (Schmidberger and Francis, 1999). The majority of the peridotites contain large crystals of olivine, orthopyroxene, clinopyroxene, and garnet and exhibit coarse textures, although a few peridotites with porphyroclastic textures are observed. Small amounts (~1% or less) of phlogopite are present, whereas amphibole is absent. The term *peridotite* is used for the mantle xenoliths in this study because the small differences in modal clinopyroxene content do not justify dividing the suite according to the International Union of Geological Sciences (IUGS) classification into harzburgites (clinopyroxene <5 wt. %) or lherzolites (clinopyroxene >5 wt. %). A detailed description of xenolith mineralogy and major, trace, and rare earth element (REE) chemistry can be found in Schmidberger and Francis (1999) and Schmidberger and Francis (2001). The estimated temperature and pressure conditions of last equilibration (800–1400°C, 25–60 kb) indicate that the Nikos peridotites were sampled at depths between 80 to 190 km by their host kimberlite (Schmidberger and Francis, 1999).

The high magnesium numbers (mg-number = Mg/(Mg + Fe) = 0.90 to 0.93) and olivine-rich mineralogy (avg. 80 wt. %) of the peridotites reflect their refractory nature and suggest that these xenoliths are melt-depleted residues (Schmidberger and Francis, 1999, 2001). In contrast to their depleted major element chemistry, however, the peridotites are enriched in LILE compared with abundances estimated for primitive mantle and LREE (La/Sm_N = 4–6) relative to chondrites, whereas the heavy rare earth element (HREE) contents are approximately chondritic (Schmidberger and Francis, 2001).

Minor pyroxenite xenoliths consisting of clinopyroxene, orthopyroxene, and garnet show a range in mg-numbers (Schmidberger and Francis, 1999). Two high-Mg pyroxenites contain olivine and abundant garnet (avg. 20 wt. %), and have mg-numbers (0.88–0.90) similar to those of the peridotites. Two low-Mg pyroxenites (mg-number = 0.85) have lower modal abundances of garnet (avg. 10 wt. %) and higher clinopyroxene contents (avg. 70 wt. %) than the high-Mg pyroxenites (avg. 30 wt. %). Both the high-Mg and low-Mg pyroxenites are enriched in incompatible trace elements, such as LILE and LREE, relative to values for primitive mantle and chondrites (Schmidberger and Francis, 2001). The low-Mg pyroxenites, however, are less enriched in incompatible trace elements than the high-Mg pyroxenites.

2.3. Clinopyroxene and Garnet

The emerald green clinopyroxenes in the Somerset peridotites are chromian diopside, and the garnets are chromian pyrope (Schmidberger and Francis, 1999). The major element compositions of both clinopyroxene and garnet are homogeneous on the scale of a thin section.

Mass balance calculations using REE contents of clinopyroxene and garnet and their respective modal abundances indicate that calculated LREE abundances for all Nikos xenoliths are significantly lower (e.g., La: 70–99%, Nd and Sm: ~50%) than those of the analyzed whole-rocks, while having similar HREE contents (Schmidberger and Francis, 2001). These results suggest the presence of a kimberlite-related LREE-rich interstitial component (i.e., ~1% kimberlite liquid), accessory mineral phase (i.e., trace amounts of apatite, although as yet undetected in thin sections), or both to account for the excess trace element abundances (Schmidberger and Francis, 2001).

The mineral trace element compositions indicate that the peridotites can be divided according to temperature and thus depth of origin into low-temperature (<1100°C; 80–150 km) and high-temperature xenoliths (>1100°C; 160–190 km). The clinopyroxenes from the low-temperature peridotites have LREE (e.g., La = 6–25 ppm) and Sr (100–400 ppm) abundances that are significantly higher than those of clinopyroxene from the high-temperature peridotites (La = 0.4–2 ppm; Sr = 50–140 ppm; Schmidberger and Francis, 2001). In addition, the calculated LREE patterns for the majority of the shallow low-temperature peridotites are flat, whereas the deep-seated, high-temperature peridotites are characterized by LREE-depleted calculated bulk rock patterns relative to chondrites (Schmidberger and Francis, 2001). These findings suggest that the shallow Somerset lithosphere is geochemically distinct from the underlying lower lithospheric mantle and that the mantle root beneath the northern Canadian craton is characterized by a depth zonation in incompatible trace elements (Schmidberger and Francis, 2001).

3. ANALYTICAL METHODS

All exterior surfaces were first removed from the xenoliths. Samples were then crushed, and rock chips were ground in an aluminum mill. Crushed whole-rock kimberlite samples were carefully handpicked under the binocular microscope before grinding to eliminate contamination from peridotite xenocrysts and country rock fragments. Garnet and clinopyroxene separates were handpicked under the binocular microscope, and inclusion free crystals were washed in an ultrasonic bath with acetone, ultrapure water, and then 2.5 N HCl.

For Nd and Sr isotope analyses, the sample powders were spiked with a mixed ^{150}Nd-^{149}Sm isotope tracer and dissolved in a mixture of HF-HNO_3-$HClO_4$. Whole-rock samples and the garnet separates were dissolved at 170°C in Teflon bombs and clinopyroxene separates at 140°C in Savillex vials for at least 10 d. Sr and REE were separated using conventional chromatographic techniques. Typical procedural blanks are Sr <70 pg, and Nd and Sm <40 pg. Sr aliquots were loaded using a TaF solution on single W filaments, and Nd and Sm were loaded with HCl using a triple Re filament technique. Nd and Sr isotope measurements were obtained by thermal ionization mass spectrometry (TIMS) at GEOTOP, Université du Québec à Montréal (UQAM), using a Sector 54 mass spectrometer operated in the static multicollection mode. For Pb isotope analysis, the sample powders were dissolved in a mixture of HF-HNO_3. Pb was separated using anion-exchange chromatography (after Manhès et al., 1980), U and Th determinations followed the technique of Edwards et al. (1986), and both were conducted at GEOTOP-UQAM. Pb, U, and Th concentrations were determined by isotope dilution using ^{206}Pb, ^{233}U-^{236}U and ^{229}Th spikes. Procedural blanks for Pb, U, and Th were 10 to 15, 2 to 6, and 80 to 100 pg, respectively, and are considered negligible. Pb aliquots were loaded on a single Re filament using a silica gel–H_3PO_4 acid mixture, and Pb isotope measurements were obtained using a single Faraday cage detector or Daly analog detector in peak switching mode. Pb, U, and Th concentrations were determined using a Micromass IsoProbe multicollector inductively coupled mass spectrometer (MC-ICP-MS) coupled to an ARIDUS microconcentric nebuliser.

4. RESULTS

4.1. Kimberlite

Initial Nd and Sr isotope data for the Nikos kimberlites were calculated for an emplacement age of 100 Ma. $^{143}Nd/^{144}Nd_{(t)}$ ratios are tightly constrained between 0.51254 and 0.51259 (corresponding to initial ε_{Nd} values of +0.6 to +1.5) and are similar to or slightly depleted than the composition of CHUR (chondrite uniform reservoir; Table 1; Fig. 2). The $^{87}Sr/^{86}Sr_{(t)}$ ratios (0.7052) are identical and are slightly "enriched" compared with the value for bulk Earth. Previous studies on South African kimberlites have divided kimberlites into two groups (Group I and Group II) based on their distinct mineralogy and isotopic signatures, indicating derivation from isotopically distinct mantle domains (Dawson, 1967; Smith, 1983). More recently, South African "Group II" kimberlites were recognized to have similar mineralogy and chemical compositions to those of olivine lamproites and were termed orangeites by Mitchell (1995). Initial Nd and Sr isotopic compositions for the Nikos kimberlites plot close to the field encompassing data for "Group I" kimberlites from North America, South Africa, and Siberia, which are undifferentiated to slightly depleted relative to values for CHUR and bulk Earth, respectively (Smith, 1983; Heaman, 1989; Pearson et al., 1995b; Fig. 2). Isotope data for South African "Group II" and Australian "kimberlites," in contrast, have much lower Nd and higher Sr isotopic ratios than the Nikos kimberlites and all "Group I" kimberlites (McCulloch et al., 1983; Smith, 1983; Fig. 2).

The Pb isotopic compositions of the Nikos kimberlites show a positive correlation in Pb-Pb isotope diagrams at the time of emplacement (Table 2; Fig. 3). The Pb isotope array yields a $^{207}Pb/^{206}Pb$ age of ~2.7 Ga but is not likely to have any geochronological significance. In an initial $^{206}Pb/^{204}Pb$ vs. $^{208}Pb/^{204}Pb$ diagram, the Nikos kimberlite Pb isotope ratios plot between data for "Group I" and "Group II" kimberlites from South Africa (Kramers, 1977; Fraser et al., 1985; Fig. 3).

Table 1. Rb, Sr, Sm, and Nd abundances and Sr and Nd isotope compositions for Nikos kimberlites and xenoliths.

Sample	Temp °C	Press kb	Rb ppm	Sr ppm	$^{87}Rb/^{86}Sr$	$^{87}Sr/^{86}Sr$ measured	$^{87}Sr/^{86}Sr$ (t)	Sm ppm	Nd ppm	$^{147}Sm/^{144}Nd$	$^{143}Nd/^{144}Nd$ measured	$^{143}Nd/^{144}Nd$ (t)	T_{DM} Ma	ε_{Nd} (t)
Kimberlites														
NK3–K1			72	1320	0.16	0.705403 ± 14	0.7052	10.1	74.6	0.0819	0.512617 ± 11	0.512563		1.1
NK3–K2			44	1030	0.12	0.705334 ± 14	0.7052	10.7	78.3	0.0828	0.512593 ± 07	0.512539		0.6
NK3–K3			30	1710	0.05	0.705248 ± 14	0.7052	14.7	110	0.0808	0.512640 ± 07	0.512587		1.5
NK3–K4			20	2190	0.03	0.705243 ± 16	0.7052	12.7	94.5	0.0814	0.512634 ± 12	0.512580		1.4
duplicate						0.705245 ± 13								
NK3–K5			31	1330	0.07	0.705272 ± 13	0.7052	11.6	82.5	0.0850	0.512631 ± 05	0.512575		1.3
Low-temperature peridotites														
NK3–20	815	29.8	7.3	55.9	0.38	0.705677 ± 10	0.7051	0.37	1.58	0.1411	0.512763 ± 11	0.512671	812	3.2
NK1–4	871	33.5	3.0	43.3	0.20	0.706917 ± 14	0.7066	0.24	1.49	0.0984	0.512676 ± 14	0.512611	628	2.0
NK1–4 Cpx			0.01[a]	115[a]	0	0.703776 ± 11	0.7038	1.38	9.50	0.0875	0.512620 ± 05	0.512562	641	1.0
NK1–4 Gt			0.02[a]	0.17	0.29	0.707539 ± 14	0.7071	0.43	0.49	0.5256	0.513049 ± 09	0.512705		3.8
NK2–3	887	34.6	7.5	77.7	0.28	0.706093 ± 14	0.7057	0.38	2.63	0.0879	0.512701 ± 12	0.512643	545	2.6
NK2–3 Cpx				318		0.704584 ± 14	0.7046	2.09	14.6	0.0864	0.512732 ± 10	0.512676	501	3.3
NK2–3 Gt				0.27		0.706887 ± 16	0.7065	0.70	1.99	0.2135	0.512829 ± 08	0.512690		3.5
NK1–23	964	39.0	4.7	86.5	0.16	0.705329 ± 11	0.7051	0.51	3.64	0.0853	0.512755 ± 10	0.512699	470	3.7
NK2–10	1014	42.1	3.0	92.6	0.09	0.705637 ± 13	0.7055	0.47	2.93	0.0964	0.512648 ± 05	0.512585	653	1.5
NK1–14	1027	42.7	1.4	43.7	0.10	0.705792 ± 14	0.7057	0.31	1.97	0.0944	0.512657 ± 13	0.512595	631	1.7
NK1–14 Cpx				217		0.703814 ± 14	0.7038	3.19	23.9	0.0806	0.512621 ± 08	0.512568	607	1.1
NK1–14 Gt				0.31		0.706495 ± 11	0.7061	1.08	2.08	0.3137	0.512807 ± 09	0.512602		1.8
NK1–2	1042	44.7	1.2	33.8	0.10	0.705534 ± 14	0.7054	0.27	1.75	0.0938	0.512655 ± 16	0.512594	630	1.6
NK1–12	1054	45.3	3.2	56.5	0.16	0.706203 ± 14	0.7060	0.40	2.21	0.1094	0.512670 ± 19	0.512599	702	1.8
NK1–3	1076	46.5	1.7	56.3	0.09	0.706668 ± 14	0.7065	0.33	1.53	0.1324	0.512655 ± 14	0.512568	928	1.2
NK1–3 Cpx				406		0.704149 ± 14	0.7041	5.60	28.0	0.1207	0.512646 ± 08	0.512567	827	1.1
NK1–3 Gt[b]				0.73		0.706472 ± 14	0.7061	1.99	2.82	0.4272	0.512829 ± 07	0.512550		0.8
NK2–4[b]			1.9	14.9	0.37	0.705188 ± 16	0.7047	0.21	0.97	0.1280	0.512847 ± 08	0.512763	541	5.0
NK2–4 Cpx				133[a]		0.703879 ± 13	0.7039	1.54	6.88	0.1357	0.512775 ± 09	0.512686	733	3.5
NK2–4 Gt[b]						0.707703 ± 13	0.7073	1.62	2.45	0.3999	0.512886 ± 11	0.512624		2.2
High-temperature peridotites														
NK1–6	1149	48.4	0.8	17.1	0.14	0.706544 ± 13	0.7064	0.22	0.97	0.1371	0.512674 ± 29	0.512584	947	1.5
NK2–1	1216	51.5	10	31.3	0.93	0.709277 ± 13	0.7080	0.14	0.66	0.1299	0.512624 ± 17	0.512539	958	0.6
duplicate						0.709286 ± 10					0.512607 ± 23			
NK2–1 Cpx				45.8		0.709132 ± 17	0.7091	0.79	2.97	0.1604	0.512664 ± 12	0.512559	1386	1.0
NK2–1 Gt			0.08[a]	0.57	0.39	0.710015 ± 14	0.7095	1.16	1.13	0.6205	0.512966 ± 17	0.512560		1.0
NK1–9	1219	53.4	1.5	17.8	0.25	0.706912 ± 13	0.7066	0.23	0.88	0.1548	0.512661 ± 21	0.512560	1264	1.0
NK1–1	1222	52.7	1.1	25.7	0.12	0.707152 ± 10	0.7070							
NK3–11	1247	53.1	2.9	202	0.04	0.708065 ± 24	0.7080	0.25	1.05	0.1405	0.512655 ± 15	0.512563	1032	1.0
NK3–25	1256	54.0	29	37.5	2.21	0.709693 ± 17	0.7066	0.33	1.76	0.1120	0.512628 ± 31	0.512554	783	0.9
NK1–5	1262	54.6	4.3	46.5	0.27	0.706955 ± 13	0.7066	0.26	1.09	0.1451	0.512694 ± 16	0.512600	1013	1.8
NK1–5 Cpx				75.0		0.706674 ± 14	0.7067	1.36	5.88	0.1395	0.512700 ± 10	0.512609	924	2.0
NK1–5 Gt[b]				0.51		0.707442 ± 14	0.7069	1.13	1.07	0.6334	0.512999 ± 09	0.512584		1.5
NK3–16	1280	53.5	1.8	40.9	0.13	0.707234 ± 13	0.7071	0.17	0.88	0.1177	0.512662 ± 10	0.512585	775	1.5
NK1–7	1300	55.1	1.0	15.2	0.20	0.706660 ± 14	0.7064	0.14	0.44	0.1904	0.512749 ± 38	0.512624	2610	2.3
NK1–7 Cpx				86.9		0.706066 ± 17	0.7061							
NK1–7 Gt				0.48		0.707249 ± 14	0.7067	1.33	1.45	0.5551	0.512886 ± 10	0.512523		0.3
NK2–2	1316	54.7	6.5	33.5	0.56	0.708523 ± 14	0.7077	0.30	1.24	0.1488	0.512686 ± 11	0.512588	1090	1.6
NK2–2 Cpx			0.01[a]	106[a]	0	0.707280 ± 13	0.7073	1.38	5.71	0.1456	0.512687 ± 10	0.512591	1037	1.6
NK2–2 Gt				0.35		0.709472 ± 14	0.7089	0.73	0.91	0.4850	0.512911 ± 10	0.512594		1.7
NK3–15	1343	58.5	3.7	344	0.03	0.708533 ± 14	0.7085	0.20	1.16	0.1043	0.512639 ± 14	0.512571	713	1.2
NK3–4	1371	58.5	23	245	0.27	0.708867 ± 13	0.7085	0.42	2.21	0.1150	0.512569 ± 21	0.512494	897	−0.3
NK 3–4 Cpx				92.7		0.705199 ± 14	0.7052	1.07	4.31	0.1501	0.512639 ± 10	0.512541	1224	0.6
Nk 3–4 Gt				0.43		0.708717 ± 14	0.7082	0.69	0.72	0.5752	0.512797 ± 10	0.512421		−1.7
Pyroxenites														
NK2–7 HMg	737	25.3	4.1	284	0.04	0.704128 ± 11	0.7041	0.80	4.98	0.0973	0.512554 ± 10	0.512490	781	−0.4
NK3–14 HMg	933	36.8	30	162	0.54	0.706629 ± 11	0.7059	1.67	8.29	0.1218	0.512720 ± 41	0.512640	714	2.6
NK3–17 LMg	720	22.2	3.6	38.8	0.27	0.706108 ± 10	0.7057	0.58	1.99	0.1745	0.512980 ± 09	0.512866	660	7.0
NK3–1 LMg	759	25.1	5.1	90.3	0.16	0.704840 ± 21	0.7046	0.67	3.05	0.1330	0.512058 ± 10	0.511971	2055	−10.5
Nk 3–1 Cpx			0.01[a]	89.4[a]	0	0.704268 ± 13	0.7043	1.06	4.77	0.1342	0.511879 ± 15	0.511791	2426	−14.0
Nk 3–1 Gt			0.02[a]	0.14	0.35	0.706110 ± 16	0.7056	0.48	0.77	0.3806	0.512956 ± 21	0.512707		3.9

Note: Minerals and rock types: *Cpx* = clinopyroxene; *Gt* = garnet; *HMg* = high-Mg pyroxenite; *LMg* = low-Mg pyroxenite. (t): Sr and Nd isotope ratios corrected for 100 Ma in situ decay. $^{87}Sr/^{86}Sr$ are normalized to $^{86}Sr/^{88}Sr = 0.1194$ and $^{143}Nd/^{144}Nd$ to $^{146}Nd/^{144}Nd = 0.7219$. NBS 987 Sr standard yielded an average value of $^{87}Sr/^{86}Sr = 0.710253 \pm 0.000013$ (2σ; $n = 10$). Measurements of Ames Nd standard gave an average value of $^{143}Nd/^{144}Nd = 0.512132 \pm 0.000011$ (2σ; $n = 8$). Precision for individual Sr and Nd isotope measurements is quoted at the 2σ level. Sm and Nd abundances were determined by isotope dilution analysis with uncertainties <0.5%. Rb and Sr abundances for bulk rocks were measured by ICP-MS analysis (for analytical procedures see Schmidberger and Francis, 2001).

[a] Rb and Sr abundances for Cpx and Gt were determined by isotope dilution analysis with uncertainties <1%, and these were used to calculate $^{87}Rb/^{86}Sr$ ratios for the remaining mineral separates (for further explanation, see text). Sr abundances for other Cpx and Gt separates were measured by ion microprobe analysis.

[b] Temperature and pressure estimates not determined.

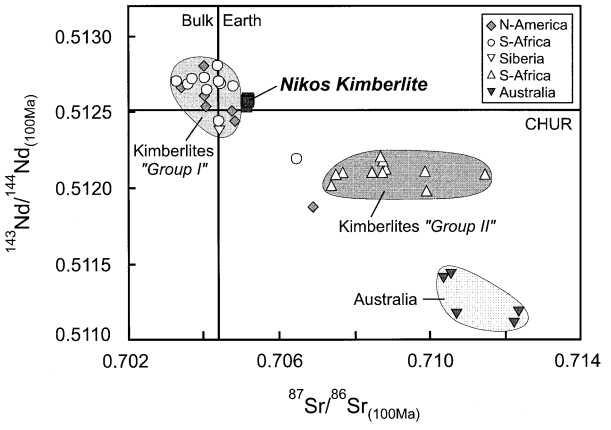

Fig. 2. Initial Nd and Sr isotopic compositions for Nikos kimberlites. The Nd and Sr isotopic ratios for kimberlites from North America, Siberia, South Africa, and Australia ("Group I" and "Group II" kimberlites; for further explanation see text) are shown for comparison (data from McCulloch et al., 1983; Smith, 1983; Heaman, 1989; Pearson et al., 1995b). Values for bulk Earth and CHUR (chondrite uniform reservoir) are those for 100 Ma ago, assuming present-day ratios of $^{87}Sr/^{86}Sr_{(bulk\ Earth)} = 0.7045$ and $^{87}Rb/^{86}Sr_{(bulk\ Earth)} = 0.083$ ($\lambda = 1.42 \times 10^{-11}\ y^{-1}$) and $^{143}Nd/^{144}Nd_{(CHUR)} = 0.512638$ and $^{147}Sm/^{144}Nd_{(CHUR)} = 0.1967$ ($\lambda = 6.54 \times 10^{-12}\ y^{-1}$).

However, South African "Group II" kimberlites exhibit lower $^{206}Pb/^{204}Pb_{(t)}$ at similar $^{207}Pb/^{204}Pb_{(t)}$ isotopic ratios than those of the Nikos and South African "Group I" kimberlites (Kramers, 1977; Smith, 1983; Fraser et al., 1985; Fig. 3).

4.2. Mantle Xenoliths

The whole-rock Nd and Sr isotopic compositions for the Nikos xenoliths were corrected for the 100 Ma in situ decay since the emplacement of their host kimberlite (Table 1). $^{143}Nd/^{144}Nd_{(t)}$ ratios of the peridotites range between 0.51249 to 0.51276 ($\varepsilon_{Nd(t)}$ values of -0.3 to $+5.0$) and are similar to or depleted relative to the value for CHUR (Fig. 4). The Nd isotopic compositions of the low-temperature peridotites extend to slightly more radiogenic values ($^{143}Nd/^{144}Nd_{(t)} = 0.51257-0.51276$) than those in the high-temperature peridotites ($^{143}Nd/^{144}Nd_{(t)} = 0.51249-0.51262$). Depleted mantle Nd model ages (T_{DM}) for the peridotites range from 500 to 1250 Ma (except NK1–7: 2600 Ma; Table 1). $^{87}Sr/^{86}Sr_{(t)}$ isotopic ratios in the peridotites show a significant variation (0.7047–0.7085) and are "enriched" relative to bulk Earth (Fig. 4). The shallow low-temperature peridotites have Sr isotopic compositions that are significantly less radiogenic ($^{87}Sr/^{86}Sr_{(t)} = 0.7047-0.7066$) than those in the high-temperature peridotites ($^{87}Sr/^{86}Sr_{(t)} = 0.7064-0.7085$; Fig. 4). The unradiogenic Sr and radiogenic Nd isotope ratios for one peridotite (NK2–4) suggest that it represents a sample of low-temperature lithosphere, although temperature and pressure estimates were not determined. One low-Mg pyroxenite (NK3–1) yields a very unradiogenic $^{143}Nd/^{144}Nd_{(t)}$ (0.51197) isotopic ratio relative to those of the other pyroxenites and the peridotites (Fig. 4).

The $^{143}Nd/^{144}Nd_{(t)}$ isotopic compositions of the low- and high-temperature peridotites are similar to those of the Nikos kimberlite, while having significantly more variable $^{87}Sr/^{86}Sr_{(t)}$ ratios (Fig. 4). The Nd and Sr isotopic signatures of all Nikos peridotites overlap the field of kimberlite-hosted garnet peridotites (including whole-rock and clinopyroxene data) from the South African craton (Menzies and Murthy, 1980; Kramers et al., 1983; Richardson et al., 1985; Jones, 1987; Walker et al., 1989; Hawkesworth et al., 1990a; Macdougall and Haggerty, 1999; Fig. 4). Although the low-temperature South African xenoliths encompass the entire garnet peridotite field, many of the high-temperature South African xenoliths appear to be slightly depleted relative to CHUR and bulk Earth. In contrast, Sr isotopic ratios for the Nikos peridotites exhibit the opposite relationship, with the most radiogenic values observed for the high-temperature xenoliths. In comparison, the Nd and Sr isotopic compositions for post-Archean spinel peridotites plot within the depleted quadrant relative to CHUR and bulk Earth, respectively, and are distinct from those for most kimberlite-hosted cratonic mantle xenoliths (Hawkesworth et al., 1990b, and references therein).

The high-temperature peridotites have μ ($^{238}U/^{204}Pb$) values that are significantly higher (avg. $\mu = 37$) than those of both the low-temperature peridotites (avg. $\mu = 25$) and the host Nikos kimberlite (avg. $\mu = 12$; Table 2). The μ values for both high- and low-temperature peridotites, however, are higher than those estimated for melt-depleted residues ($\mu \sim 10$; Zindler and Hart, 1986; Fig. 5), suggesting the preferential addition of U after lithosphere formation. The Nikos Pb isotopic ratios plot below the Stacey and Kramers (1975) lead isotope evolution curve ($\mu = 9.7$) and dominantly to the right of the geochron (Fig. 5). The high-temperature peridotites exhibit $^{206}Pb/^{204}Pb_{(t)}$ (17.181–18.299) isotopic compositions that are less radiogenic than those of the low-temperature peridotites ($^{206}Pb/^{204}Pb_{(t)} = 17.820-19.033$), whereas their $^{207}Pb/^{204}Pb_{(t)}$ and $^{208}Pb/^{204}Pb_{(t)}$ ratios are indistinguishable (Table 2; Fig. 5). The Pb isotopic signatures for the Nikos peridotites partly overlap those for the Nikos kimberlites at the time of emplacement (Fig. 5), and both the low- and high-temperature Nikos peridotites have Pb isotopic compositions that are within the range of previously reported data for garnet peridotites (including whole-rock and clinopyroxene data) in South African kimberlites (Kramers, 1977; Kramers et al., 1983; Richardson et al., 1985; Walker et al., 1989; Hawkesworth et al., 1990a; Fig. 5).

The Pb isotopic ratios of the one high-Mg pyroxenite are similar to those of the peridotites. One low-Mg pyroxenite (NK3–1) is characterized by very unradiogenic Pb isotopic compositions ($^{206}Pb/^{204}Pb_{(t)} = 16.91$), whereas the other (NK3–17) has highly radiogenic Pb isotopic ratios ($^{206}Pb/^{204}Pb_{(t)} = 19.61$; Fig. 5).

4.3. Clinopyroxene and Garnet

The Nd isotopic ratios of clinopyroxene in the Nikos peridotites are depleted relative to the value for CHUR (Table 1; Fig. 6). Although the Nd isotopic compositions mostly overlap, two clinopyroxenes from the low-temperature peridotites ($^{143}Nd/^{144}Nd_{(t)} = 0.51268-0.51269$) exhibit more radiogenic values than those of clinopyroxenes from the high-temperature xenoliths ($^{143}Nd/^{144}Nd_{(t)} = 0.51254-0.51261$). Depleted mantle Nd model ages (T_{DM}) yield 500 to 800 Ma and 900 to 1400 Ma for clinopyroxenes from low- and high-temperature peridotites, respectively. Rb and Sr abundances for Nikos clinopy-

'Table 2. Pb, U, and Th abundances and Pb isotopic compositions for Nikos kimberlites and xenoliths.

Sample	Pb ppm	U ppm	Th ppm	$^{238}U/^{204}Pb$ μ	$^{206}Pb/^{204}Pb$ measured	$^{207}Pb/^{204}Pb$ measured	$^{208}Pb/^{204}Pb$ measured	$^{206}Pb/^{204}Pb$ (t)	$^{207}Pb/^{204}Pb$ (t)	$^{208}Pb/^{204}Pb$ (t)
					Kimberlites					
NK3–K1	11	2.9	14.4	17.0	18.485	15.478	38.584	18.220	15.465	38.151
NK3–K2	14	3.2	14.1	14.6	18.483	15.466	38.699	18.255	15.455	38.367
NK3–K3	14	3.5	18.5	16.2	18.712	15.512	38.903	18.458	15.500	38.466
NK3–K4	28	3.8	17.5	8.8	18.758	15.513	38.906	18.621	15.506	38.700
NK3–K5	35	2.9	14.1	5.4	18.704	15.537	38.899	18.619	15.533	38.766
average	*20*	*3.3*	*15.7*	*12.4*						
					Low-Temperature Peridotites					
NK3–20	0.08	0.03	0.08	22.2	18.823	15.587	38.815	18.476	15.570	38.496
NK1–4	0.22	0.08	0.22	22.7	18.675	15.542	38.654	18.320	15.525	38.315
NK2–3	0.27	0.16	0.32	36.7	19.147	15.509	38.953	18.573	15.481	38.568
NK1–23	0.07	0.04	0.07	30.7	18.600	15.451	38.316	18.120	15.428	37.997
NK2–10	0.66	0.17	0.30	16.3	19.287	15.550	38.556	19.033	15.538	38.405
NK1–14	0.14	0.06	0.26	28.3	18.771	15.517	38.771	18.328	15.496	38.166
NK1–2	0.15	0.04	0.15	18.5	18.587	15.494	38.545	18.298	15.480	38.209
NK1–12	0.26	0.06	0.21	15.1	18.798	15.515	38.540	18.563	15.504	38.269
NK1–3	0.17	0.10	0.16	37.5	18.407	15.394	38.128	17.820	15.366	37.818
NK2–4	0.08	0.03	0.07	21.9	18.994	15.503	38.759	18.652	15.487	38.435
average	*0.21*	*0.08*	*0.18*	*25.0*						
					High-Temperature Peridotites					
NK2–1	0.09	0.02	0.06	14.8	18.520	15.427	38.386	18.288	15.416	38.157
NK1–9	0.10	0.03	0.08	20.2	18.614	15.496	38.521	18.299	15.481	38.232
NK1–1	0.14	0.08	0.13	37.7	18.571	15.454	38.404	17.981	15.426	38.109
NK3–11	0.58	0.69	0.10	77.6	19.193	15.575	38.645	17.980	15.516	38.586
NK3–25	0.42	0.37	0.16	56.6	18.314	15.436	38.286	17.430	15.394	38.158
NK1–5	0.24	0.08	0.12	20.3	18.426	15.492	38.337	18.109	15.476	38.168
NK3–16	0.29	0.21	0.08	46.3	18.377	15.549	38.531	17.654	15.515	38.442
NK1–7	0.04	0.01	0.05	17.2	18.494	15.509	38.320	18.225	15.496	37.914
NK2–2	0.17	0.08	0.06	28.6	18.682	15.472	38.203	18.236	15.450	38.082
NK3–4	0.33	0.48	0.11	93.4	18.641	15.455	38.288	17.181	15.385	38.181
average	*0.21*	*0.17*	*0.10*	*37.1*						
					Pyroxenites					
NK2–7 HMg	1.99	0.35	0.49	11.5	18.964	15.509	38.756	18.785	15.500	38.675
NK3–17 LMg	0.75	0.13	0.33	11.6	19.788	15.632	38.860	19.607	15.623	38.715
NK3–1 LMg	0.39	0.04	0.14	6.6	17.015	15.349	37.285	16.912	15.344	37.169

Note: Rock types: *HMg* = high-Mg pyroxenite; *LMg* = low-Mg.pyroxenite.(t): Pb isotope ratios corrected for 100 Ma in situ decay. Mass fractionation corrections of 0.09% amu^{-1} and 0.24% amu^{-1} were applied to Pb isotope ratios (based on repeated measurements of NIST SRM 981 Pb standard) using Faraday and Daly analogue detectors, respectively. Average values for the internal precision (2σ) of the $^{206}Pb/^{204}Pb$, $^{207}Pb/^{204}Pb$, and $^{208}Pb/^{204}Pb$ ratios are ±0.016, ±0.014, and ±0.038, respectively). Pb, U, and Th abundances for xenoliths were determined by isotope dilution analysis with uncertainties $<1\%$ and for kimberlites by ICP-MS analysis (for analytical procedures see Schmidberger and Francis, 2001).

roxene separates from two peridotites and one pyroxenite were determined using isotope dilution analysis (Table 1). Because the calculated $^{87}Rb/^{86}Sr$ ratios are extremely low (high-temperature peridotite: 0.00020; low-temperature peridotite: 0.00018), the correction of the measured Sr isotopic ratios for in situ decay (100 Ma) is negligible (Table 1). The $^{87}Sr/^{86}Sr_{(t)}$ ratios for the remaining clinopyroxene separates were calculated using $^{87}Rb/^{86}Sr$ ratios of 0.00020 and 0.00018 for high- and low-temperature peridotites, respectively. The Sr isotopic ratios for clinopyroxenes in the low-temperature peridotites ($^{87}Sr/^{86}Sr_{(t)} = 0.7038–0.7046$) are similar or less radiogenic than the value for bulk Earth (Fig. 6), and they are significantly less radiogenic than their corresponding whole-rock compositions (Table 1). Their Nd and Sr isotopic ratios plot within the array of data for clinopyroxenes in kimberlite-hosted peridotites from South Africa (Menzies and Murthy, 1980; Kramers et al., 1983; Jones, 1987). In contrast, the clinopyroxenes from the high-temperature Nikos peridotites exhibit a large range in Sr isotope compositions ($^{87}Sr/^{86}Sr_{(t)} = 0.7052$ to 0.7091; Fig. 6, which are significantly more radiogenic than those of the clinopyroxenes from the low-temperature peridotites.

The garnets from the low-temperature peridotites have Nd isotopic ratios ($^{143}Nd/^{144}Nd_{(t)} = 0.51255–0.51271$) that extend to slightly more radiogenic compositions than those of garnets from the high-temperature peridotites ($^{143}Nd/^{144}Nd_{(t)} = 0.51242–0.51259$; Table 1; Fig. 6) at the time of kimberlite emplacement. $^{87}Rb/^{86}Sr$ ratios for a high- (0.39) and a low-temperature peridotite garnet (0.29) were determined by isotope dilution analysis and used to calculate Sr isotopic ratios at 100 Ma ago for the remaining garnets from low- and high-temperature peridotites, respectively. The Sr isotopic compositions of garnets in the high-temperature peridotites ($^{87}Sr/^{86}Sr_{(t)} = 0.7067–0.7095$) partly overlap those of garnets in the low-temperature peridotites ($^{87}Sr/^{86}Sr_{(t)} = 0.7061–0.7073$; Table 1; Fig. 6) but extend to significantly more radiogenic values.

5. DISCUSSION

5.1. Mantle Isotopic Composition

The Nikos peridotites that sample the Archean mantle root beneath the northern Canadian craton have a refractory mineralogy with high mg-numbers and depletions in fusible major

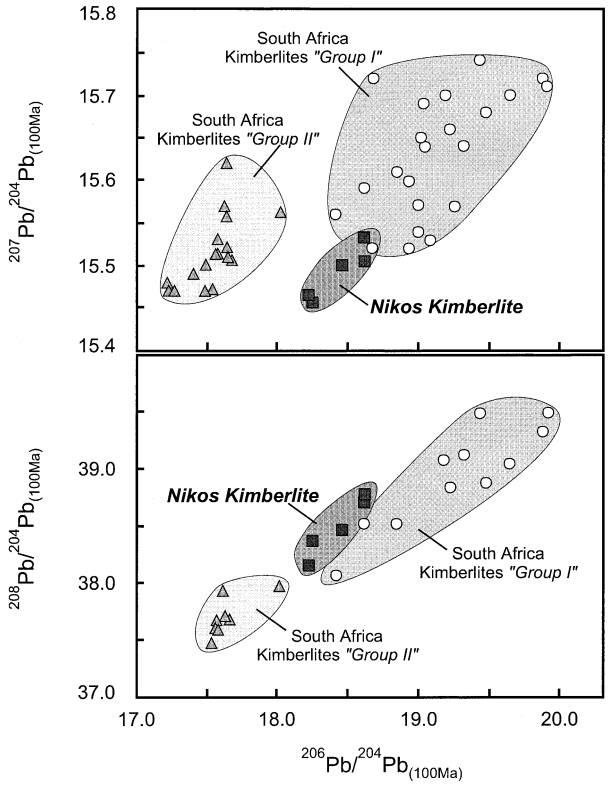

Fig. 3. Initial Pb isotopic compositions for Nikos kimberlites. The Pb isotopic ratios for South African "Group I" and "Group II" kimberlites are shown for comparison (data from Kramers, 1977; Smith, 1983; Fraser et al., 1985).

elements, indicating that they represent melt-depleted residues (Schmidberger and Francis, 1999). Residual mantle having experienced melt extraction should be characterized by low Nd/Sm, Rb/Sr, and U/Pb ratios because these trace elements are fractionated during partial melting processes (Menzies, 1990). Such trace element signatures will consequently generate time-integrated high $^{143}Nd/^{144}Nd$, low $^{87}Sr/^{86}Sr$, low $^{206}Pb/^{204}Pb$, and low $^{207}Pb/^{204}Pb$ isotopic ratios distinct from the composition of bulk Earth but similar to those of "depleted mantle" (Zindler and Hart, 1986; Menzies, 1990; Pearson et al., 1995a). In agreement with this reasoning, many spinel peridotites that sample the lithosphere beneath oceanic or post-Archean crustal terranes have Nd and Sr isotopic compositions that plot in the depleted quadrant of the Nd-Sr correlation diagram compared with CHUR and bulk Earth, respectively (Fig. 4), as would be expected for residual mantle (Hawkesworth et al., 1990b and references therein).

In contrast to their depleted major element chemistry, the Nikos peridotites are enriched in highly incompatible trace elements such as the LILE and LREE, resulting in Nd/Sm, Rb/Sr, and U/Pb ratios that are higher than those expected for melt-depleted residues (Menzies, 1990; Schmidberger and Francis, 2001; Tables 1 and 2). The Nikos peridotites have Nd isotopic compositions that are similar to that of CHUR but show a significant range in Pb and Sr isotopic compositions and extend to very radiogenic $^{87}Sr/^{86}Sr_{(t)}$ at the time of kimberlite emplacement (Figs. 4 and 5). Furthermore, the isotopic compositions of the peridotites do not correlate with indices of partial melting, such as mg-numbers or modal mineralogy, which is inconsistent with an origin as single-stage, melt-depleted residues. These characteristics suggest that the Somerset mantle root was infiltrated by metasomatic melts or fluids that enriched the lithospheric mantle in incompatible trace elements and overprinted its isotopic composition. Kimberlite-hosted garnet peridotites that sample the Archean mantle root beneath the South African Kaapvaal craton also exhibit highly variable and "enriched" isotope signatures, a feature that appears to characterize the lithospheric mantle beneath many Archean continents (Figs. 4 and 5 Hawkesworth et al., 1990b and references therein).

Mass balance calculations based on modal abundances of clinopyroxene and garnet and their respective REE abundances indicate discrepancies between calculated and analyzed LREE contents for the Nikos bulk rocks (Schmidberger and Francis, 2001). The LREE deficiencies (~50% for Nd and Sm) suggest the presence of small amounts of a kimberlite-related LREE-rich interstitial component (i.e., kimberlite liquid, ~1 wt. %) or accessory mineral phase (i.e., apatite, ~0.1 wt. %) to account for the excess LREE abundances in the Nikos peridotites (Bedini and Bodinier, 1999; Schmidberger and Francis, 2001). The Nd isotopic compositions of both the low- and high-temperature Nikos peridotites overlap those of the host kimberlite at 100 Ma ago (Fig. 4), and it would appear that the peridotites were contaminated by the Nikos kimberlite. Binary mixing calculations show that a "depleted mantle" endmember ($^{143}Nd/^{144}Nd > 0.5132$; Nd = 0.8 ppm; Zindler and Hart, 1986) would require the addition of 5 to 10 wt. % kimberlite liquid to account for the Nd isotopic signatures observed in the Nikos bulk rocks. This extent of contamination with kimberlite liquid, however, would result in bulk rock Nd abundances (5–10 ppm) that are significantly higher than those observed in the Nikos peridotites (avg. 1.5 ppm).

The presence of a Nd-bearing phase in addition to clinopyroxene and garnet is also required to explain the observation that a few whole-rock Nd isotopic compositions are less radiogenic than those of their constituent clinopyroxene and garnet. Isotopic mass balance calculations show that minor amounts of interstitial kimberlite liquid (0.5–0.9 wt. %) could explain this discrepancy. One peridotite (NK3–4), however, exhibits a whole-rock Nd isotopic composition that is in fact lower than those of the kimberlite, which suggests the presence of a grain boundary component (or accessory mineral) other than kimberlite liquid. Although the Nd isotope data and Nd contents suggest addition of small amounts of kimberlite liquid (~1 wt. % or less) or a kimberlite-related accessory mineral (apatite ~0.1 wt. % or less), binary mixing calculations indicate that the Nikos peridotites were characterized by Nd isotopic compositions that were less radiogenic than those of a typical "depleted mantle" at the time of kimberlite magmatism.

The large range in Pb isotope ratios and the trend toward extremely radiogenic Sr compositions of the high-temperature peridotites, however, cannot be explained by kimberlite ($^{87}Sr/^{86}Sr_{(t)} = 0.7052$) contamination of a precursor "depleted mantle" ($^{87}Sr/^{86}Sr < 0.703$) because the kimberlite does not have an appropriate isotopic composition to account for the Sr isotope range of the peridotites. The presence of substantial amounts (>5 wt. %) of interstitial kimberlite would in fact eradicate the

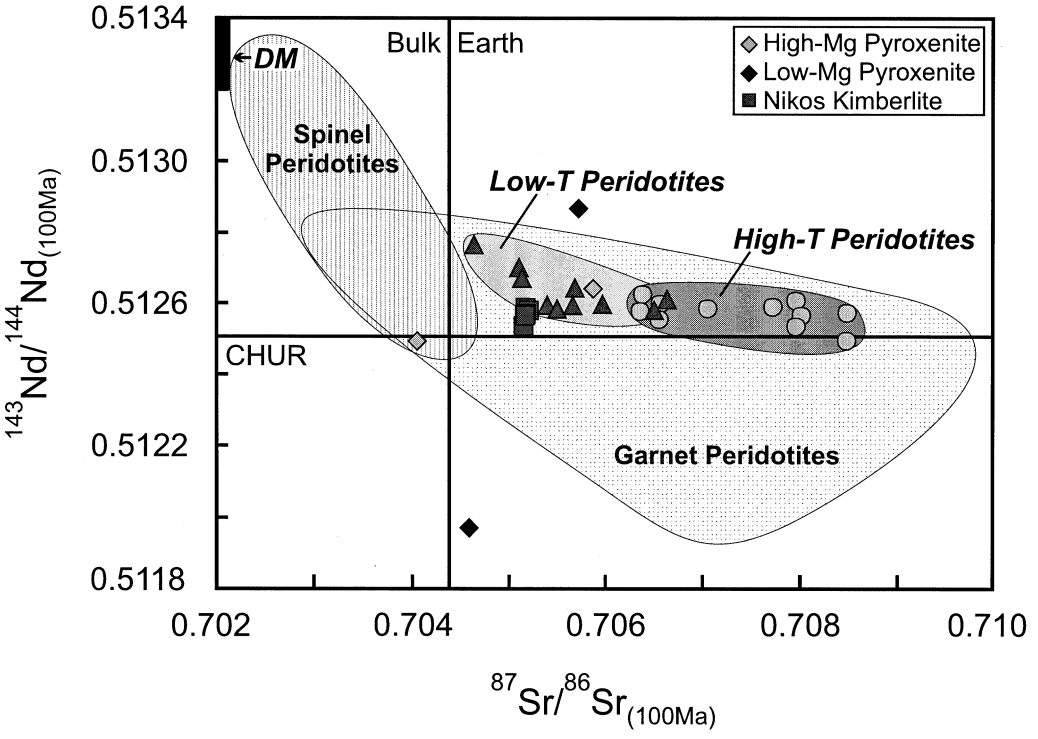

Fig. 4. Nd and Sr isotopic compositions for Nikos xenoliths at 100 Ma ago. The Nd and Sr isotopic ratios for the Nikos kimberlites, and the fields for garnet peridotites (including whole-rock and clinopyroxene data) from South African kimberlites and spinel peridotites worldwide are shown for comparison (data from Menzies and Murthy, 1980; Kramers et al., 1983; Richardson et al., 1985; Jones, 1987; Walker et al., 1989; Hawkesworth et al., 1990a,b; Macdougall and Haggerty, 1999 and references therein).

Sr and Pb isotope differences observed between the low- and high-temperature peridotites. Although Sr and Pb isotopic compositions of the high-temperature peridotites correlate with their respective Sr and Pb bulk rock abundances, which could be indicative of binary mixing of isotopically distinct components, their isotope data do not trend toward the composition of the Nikos kimberlite. This suggests that addition of host kimberlite was restricted to very small amounts (~1 wt. % or less; Fig. 7), which is consistent with previous estimates. Given any amount of kimberlite contamination, the Sr isotopic compositions of the peridotites will be affected to a lesser degree than their Nd isotope ratios because the abundance ratio (peridotite/kimberlite) of Sr is 3 times larger than for Nd.

5.1.1. Age constraints

Clinopyroxene, garnet, and corresponding whole-rock of one low (NK1–3) and two high-temperature (NK1–5; NK2–2) Nikos peridotites define internal Sm-Nd isochron ages of 91 ± 9 Ma, 94 ± 5 Ma, and 102 ± 8 Ma, respectively, essentially identical to the emplacement age of the Somerset kimberlites (Heaman, 1989; Smith et al., 1989). These young "dates" appear to represent cooling ages and suggest that the lithospheric temperatures (up to 1400°C) exceeded the closure temperatures of peridotite minerals or that Nd isotopes equilibrated (i.e., "resetting") during the thermal event associated with kimberlite magmatism. Thus, Sm-Nd isochrons using constituent peridotite minerals do not appear to provide information on the timing of stabilization of the lithospheric mantle but "date" the kimberlite magmatism. These findings are consistent with internal mineral isochrons obtained for South African peridotites, which have been interpreted to date kimberlite emplacement rather than mantle root formation (Pearson et al., 1995a).

Nd model ages may provide time constraints on separation from a depleted mantle (T_{DM}) reservoir, on the condition that bulk rock Sm-Nd systematics remain undisturbed subsequent to the formation event (DePaolo and Wasserburg, 1976). The T_{DM} (500–950 and 700–1250 Ma for low and high-temperature peridotites, respectively) for most Nikos peridotites are much younger than the Archean Re depletion ages for other Somerset Island peridotites (Irvine et al., 1999). These could reflect recent perturbation of the bulk rock Sm/Nd ratios as a result of kimberlite contamination. It has been shown that the Nd isotopic composition of clinopyroxene, which un-like that of the bulk xenolith is not biased by the presence of interstitial phases, provides a reasonable approximation for the whole-rock Nd isotope evolution (Pearson, 1999). T_{DM} age calculations yield 500 to 800 Ma (avg. 700 Ma) and 900 to 1400 Ma (avg. 1150 Ma) for clinopyroxenes from low and high-temperature peridotites, respectively, which are also significantly younger than the stabilization age of the lithosphere.

5.2. Pyroxenites

Two low-Mg pyroxenites, possibly representing veins of pyroxene-rich cumulates in the Somerset lithosphere (Schmid-

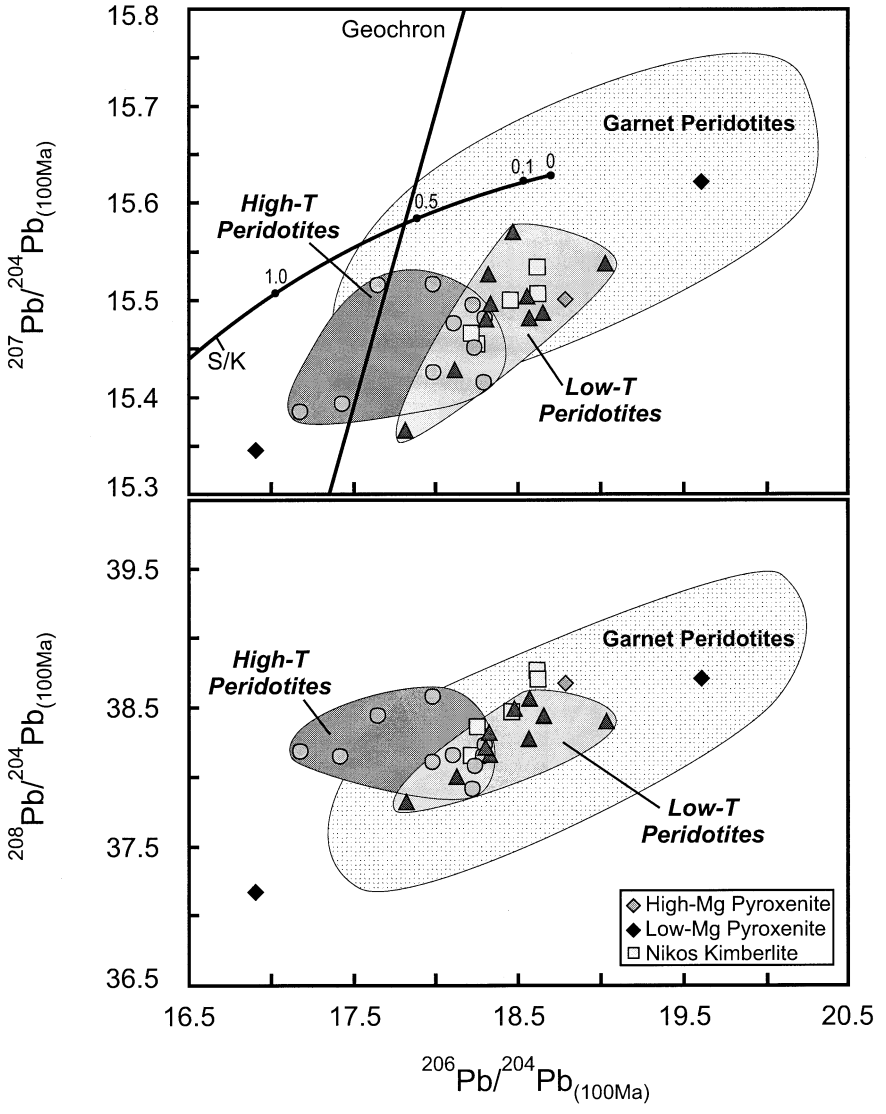

Fig. 5. Pb isotopic compositions for Nikos xenoliths at 100 Ma ago. The Pb isotopic ratios for the Nikos kimberlites and the field for kimberlite-hosted garnet peridotites (including whole-rock and clinopyroxene data) from South Africa are shown for comparison (data from Kramers, 1977; Kramers et al., 1983; Richardson et al., 1985; Walker et al., 1989; Hawkesworth et al., 1990a). S/K: Stacey and Kramers (1975) lead isotope evolution curve (time intervals in Ga).

berger and Francis, 2001), have isotopic compositions that extend from very unradiogenic (NK3–1) to highly radiogenic (NK3–17) Pb and Nd isotopic ratios, which are distinct from those of the high-Mg pyroxenites and the peridotites (Figs. 4 and 5). Thus, although major element compositions and modal mineralogy of the low-Mg pyroxenites are indistinguishable (Schmidberger and Francis, 2001), their isotopic compositions suggest that there is no genetic link between these pyroxenites. The Pb and Nd isotope signatures for one of these low-Mg pyroxenites (NK3–1) indicate that parts of the Somerset lithosphere are characterized by very low U/Pb, Th/Pb, and Sm/Nd ratios (possibly ancient feature >1Ga) to preserve such unradiogenic Pb and Nd isotopic compositions. In contrast, the high-Mg pyroxenites have Pb and Nd isotopic compositions that are similar to those of the peridotites. These pyroxenites have been interpreted to constitute a pyroxene-rich component in the lithospheric mantle produced by small-scale segregation of peridotite compositions into olivine- and pyroxene-rich layers (Schmidberger and Francis, 2001).

5.3. Isotopic Mantle Stratification

The large range in Sr and Pb isotopic ratios observed in the Nikos peridotites and the trend toward significantly higher $^{87}Sr/^{86}Sr_{(t)}$ and lower $^{206}Pb/^{204}Pb_{(t)}$ isotopic ratios for the high-temperature peridotites (Figs. 4 and 5) indicate that the deep Somerset lithosphere (>160 km) is isotopically distinct from the shallow lithospheric mantle. These findings imply that the mantle root beneath the northern Canadian craton is characterized by a depth stratification in isotopic composition that predates kimberlite magmatism at 100 Ma ago. This is in good agreement with the vertical zonation suggested by incompatible

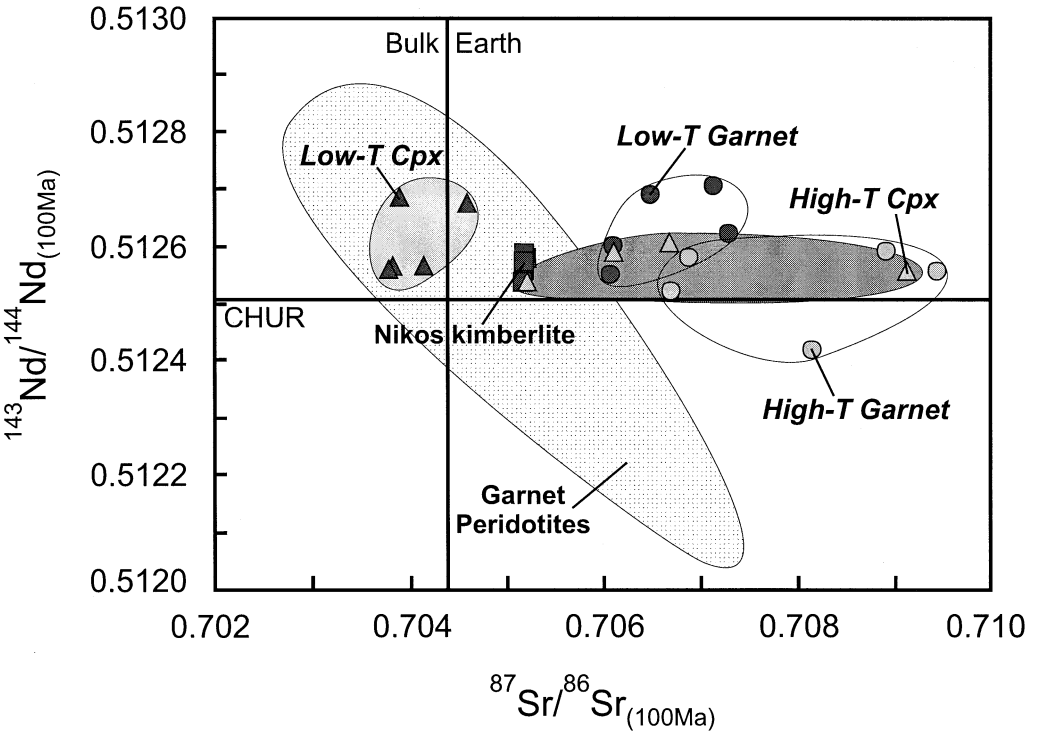

Fig. 6. Nd and Sr isotopic compositions for Nikos clinopyroxenes and garnets at 100 Ma ago. The Nd and Sr isotopic ratios for the Nikos kimberlites and the field for clinopyroxenes from kimberlite-hosted peridotites from South Africa are shown for comparison (data from Menzies and Murthy, 1980; Kramers et al., 1983; Jones, 1987).

trace element compositions of the Nikos peridotites and the decrease in trace elements contents with depth in the Somerset lithosphere (Schmidberger and Francis, 2001).

The Nikos whole-rock compositions are characterized by significantly more radiogenic Sr values than those of their constituent clinopyroxenes, a feature that is most evident in the low-temperature xenoliths. This is inconsistent with isotopic mass balance calculations using solely clinopyroxene and garnet as Sr-bearing minerals, which predict that the whole-rock Sr isotopic composition should plot close to that of clinopyroxene because it controls the bulk Sr budget. The radiogenic Sr isotope ratios of the Nikos whole-rocks, therefore, require the presence of an accessory phase (in addition to the kimberlite contaminant), most likely phlogopite, characterized by a radiogenic Sr isotopic composition ($^{87}Sr/^{86}Sr > 0.75$; Kramers et al., 1983). Small amounts of phlogopite are present in the Nikos peridotites, thus contributing to their bulk rock Sr isotope budgets and most probably responsible for the radiogenic $^{87}Sr/^{86}Sr_{(t)}$ of the xenoliths.

5.3.1. Clinopyroxene Sr isotope depth zonation

The determination of the Sr isotope compositions in inclusion-free clinopyroxene permits an unbiased isotopic characterization of the mantle lithosphere, unaffected by the presence of interstitial or accessory phases. Furthermore, the Nikos clinopyroxenes are characterized by extremely low Rb/Sr ratios ($^{87}Rb/^{86}Sr < 0.0002$), thus their present-day Sr isotope ratios are almost identical to those at the time of kimberlite emplacement because the correction for 100 Ma in situ decay is negligible.

The clinopyroxenes from the low-temperature Nikos xenoliths have Sr isotopic compositions that are less radiogenic than or similar to the composition of bulk Earth (Zindler and Hart, 1986) and are distinct from those of the Nikos kimberlite (Fig. 6). In contrast, the clinopyroxenes from the high-temperature peridotites have Sr isotopic ratios that are significantly more radiogenic than those of the Nikos kimberlite (Fig. 6). The distinct Sr isotope compositions of clinopyroxenes in the low- and high-temperature peridotites exhibit a correlation with pressures and thus depths of last equilibration (Fig. 8), in agreement with the whole-rock data (Table 1; Figs. 4 and 5), indicating that the shallow Somerset mantle is isotopically distinct from the deep lithosphere. The vertical stratification could have resulted from infiltration of the lower lithosphere with metasomatic melts or fluids originating from deeper levels of the upper mantle. This model, however, cannot be reconciled with the significantly lower Sr (and LREE) abundances of clinopyroxene from the deep-seated peridotites relative to those from the shallow peridotites (Schmidberger and Francis, 2001) as contamination with metasomatic melts or fluids should also increase their incompatible trace element abundances. The significantly more radiogenic Sr isotopic ratios and low incompatible trace element abundances of clinopyroxene in the high-temperature peridotites indicate that the shallow and deep Somerset lithosphere do not share a common petrogenetic history. It is thus possible that the deep lithospheric mantle is younger and was added to the existing shallow lithosphere by

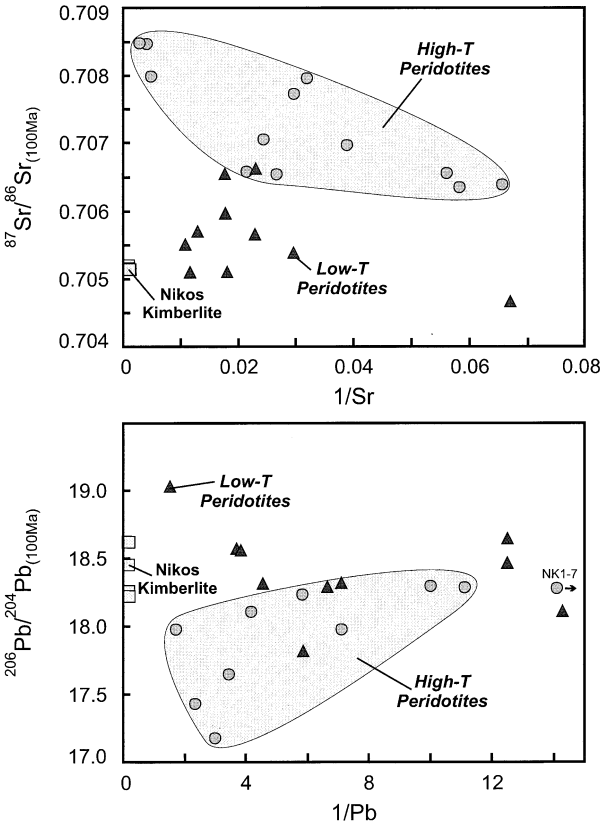

Fig. 7. Sr and Pb isotopic compositions vs. 1/Sr and 1/Pb for low- and high-temperature Nikos peridotites at 100 Ma ago. Data for the Nikos kimberlites at 100 Ma are shown for comparison.

downward growth of the mantle root during a later magmatic event (e.g., Pearson, 1999). Mantle stratification and post-Archean lithosphere growth have previously been proposed for the South African Kaapvaal craton (e.g., Menzies, 1990; Pearson et al., 1995a), and recently garnet xenocryst compositions have been interpreted to indicate that the deep lithosphere beneath the Canadian Slave craton represents underplated mantle (Griffin et al., 1999). The respective correlations of Sr and Pb isotopes with Sr and Pb abundances in the deep-seated Nikos peridotites (Fig. 7) suggest that the mantle, which underplated the shallow Somerset lithosphere, contained recycled material (altered oceanic crust and sedimentary component?; e.g., Hauri et al., 1993) characterized by radiogenic Sr and unradiogenic Pb isotopic compositions that were mixed into the mantle during earlier subduction. Recycling of oceanic lithosphere may have been related to an early Paleozoic subduction regime reported for the Canadian Arctic (Trettin et al., 1991), which would suggest that the deep Somerset lithosphere was added in the Phanerozoic.

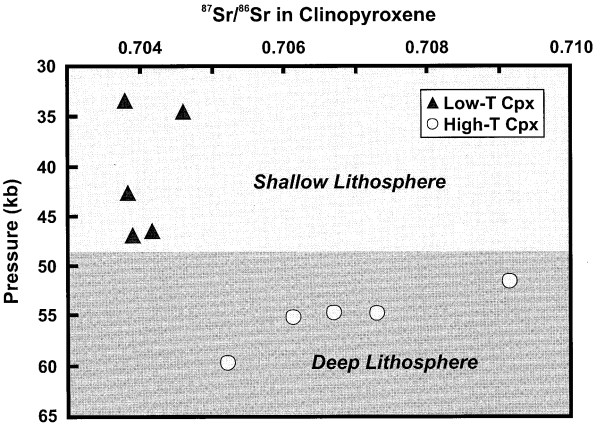

Fig. 8. Sr isotopic compositions for Nikos clinopyroxenes plotted vs. pressure of last equilibration. For sample NK2–4, pressure of last equilibration was not determined and is plotted in the lower portion of the shallow lithosphere.

The enrichment in highly incompatible trace elements observed for the low-temperature Nikos peridotites and constituent clinopyroxenes and Sr, Nd, and Pb isotopic signatures that are distinct from those for "depleted mantle" indicate that the Archean shallow lithosphere was affected by the infiltration of metasomatic melts or fluids. Although the timing of this metasomatism is difficult to constrain, it would appear to have occurred before the addition of the deep high-temperature portion of the lithosphere because the latter is less enriched in incompatible trace elements. Depleted mantle Nd model ages (T_{DM}) for clinopyroxene from the low-temperature peridotites (~700 Ma) probably indicate the maximum age for the metasomatism that affected the shallow lithosphere, which could thus have occurred as early as the late Proterozoic. A Proterozoic orogeny is recognized in the Canadian Arctic at ~700 Ma (Trettin et al., 1991), and it is possible that metasomatism of the shallow lithosphere beneath Somerset Island occurred during this event.

6. CONCLUSIONS

The Archean Nikos peridotites are characterized by a refractory olivine-rich mineralogy and major element chemistry. Nd isotopic compositions are similar or slightly depleted relative to CHUR, whereas a significant range in Sr and Pb isotope compositions is recorded, which do not correlate with the degree of major element depletion in the bulk rocks. These geochemical signatures are inconsistent with formation of the Somerset mantle root by single-stage melt extraction in the Archean because this process would generate a residual lithosphere with isotopic characteristics similar to that of "depleted mantle." The Nd isotopic ratios of the peridotites overlap those of the Nikos kimberlite, suggesting that the xenoliths were contaminated with kimberlite or a kimberlite-related accessory phase (i.e., apatite). The large range in Sr and Pb isotopic ratios observed in the xenoliths, however, indicate that addition of host kimberlite was restricted to very small amounts (~1 wt. % or less).

The high-temperature (>1100°C) Nikos peridotites that sample the deep lithospheric mantle are characterized by more radiogenic $^{87}Sr/^{86}Sr_{(t)}$ and less radiogenic $^{206}Pb/^{204}Pb_{(t)}$ isotopic signatures than those of the shallow low-temperature peridotites (<1100°C). These whole-rock data are consistent with significantly less radiogenic Sr isotopic compositions for clinopyroxenes from the low-temperature peridotites than those for clinopyroxenes from the high-temperature peridotites. The depth correlation of Sr isotopes in clinopyroxene, and Sr and Pb isotopic compositions in the Nikos whole-rocks indicate that

the deep (>160 km) and shallow Somerset lithosphere do not share the same formational history. The deep-seated, high-temperature peridotites may have been added to the existing shallow lithosphere in a Phanerozoic magmatic event, and this mantle could have contained recycled (altered oceanic crust and sedimentary component?) material as a result of earlier subduction.

Acknowledgments—We thank Fabien Rasselet for assistance in the field and for handpicking separates of magmatic kimberlite for isotope analysis. Clément Gariépy is thanked for earlier revisions of the manuscript. The research was funded by an NSERC operating grant to D. Francis, and S. Schmidberger is grateful for financial support in the form of a NSERC doctoral scholarship.

Associate editor: M. A. Menzies

REFERENCES

Bedini R. M. and Bodinier J.-L. (1999) Distribution of incompatible trace elements between the constituents of spinel peridotite xenoliths: ICP-MS data from the East African Rift. *Geochim. Cosmochim. Acta* **63,** 3883–3900.

Boyd F. R., Pokhilenko N. P., Pearson D. G., Mertzman S. A., Sobolev N. V. and Finger L. W. (1997) Composition of the Siberian cratonic mantle: Evidence from Udachnaya peridotite xenoliths. *Contrib. Mineral. Petrol.* **128,** 228–246.

Dawson J. B. (1967) A review of the geology of kimberlite. In *Ultramafic and Related Rocks* (ed. P. J. Wyllie), pp. 241–251. Wiley, New York.

DePaolo D. J. and Wasserburg G. J. (1976) Inferences about magma sources and mantle structure from variations of $^{143}Nd/^{144}Nd$. *Geophys. Res. Lett.* **3,** 743–746.

Edwards R. L., Chen J. H., and Wasserburg G. J. (1986) ^{238}U-^{234}U-^{230}Th-^{232}Th systematics and the precise measurement of time over the past 500,000 years. *Earth Planet. Sci. Lett.* **81,** 175–192.

Erlank A. J., Waters F. G., Hawkesworth C. J., Haggerty S. E., Allsopp H. L., Rickard R. S., and Menzies M. A. (1987) Evidence for mantle metasomatism in peridotite nodules from the Kimberley pipes, South Africa. In *Mantle Metasomatism* (eds. M. A. Menzies and C. J. Hawkesworth), pp. 221–311. Academic Press, London.

Fraser K. J., Hawkesworth C. J., Erlank A. J., Mitchell R. H., and Scott-Smith B.H. (1985) Sr, Nd, and Pb isotope and minor element geochemistry of lamproites and kimberlites. *Earth Planet. Sci. Lett.* **76,** 57–70.

Frisch T. and Hunt P. A. (1993) Reconnaissance U-Pb geochronology of the crystalline core of the Boothia Uplift, District of Franklin, Northwest Territories. In *Radiogenic age and isotope studies: Report 7*, pp. 3–22. Geological Survey of Canada, Paper **93–2**.

Griffin W. L., Doyle B. J., Ryan C. G., Pearson N. J., O'Reilly S. Y., Davies R., Kivi K., van Achterbergh E., and Natapov L. M. (1999) Layered mantle lithosphere in the Lac de Gras area, Slave craton: Composition, structure and origin. *J. Petrol.* **40,** 705–727.

Hauri E. H., Shimizu N., Dieu J. J. and Hart S. R. (1993) Evidence for hotspot-related carbonatite metasomatism in the oceanic upper mantle. *Nature.* **365,** 221–227.

Hawkesworth C. J., Erlank A. J., Kempton P. D., and Waters F. G. (1990a) Mantle metasomatism: Isotope and trace-element trends in xenoliths from Kimberley, South Africa. *Chem. Geol.* **85,** 19–34.

Hawkesworth C. J., Kempton P. D., Rogers N. W., Ellam R. M., and van Calsteren P. W. (1990b) Continental mantle lithosphere, and shallow level enrichment processes in the Earth's mantle. *Earth Planet. Sci. Lett.* **96,** 256–268.

Heaman L. H. (1989) The nature of the subcontinental mantle from Sr-Nd-Pb isotopic studies on kimberlite perovskite. *Earth Planet. Sci. Lett.* **92,** 323–334.

Herzberg C. T. (1993) Lithosphere peridotites of the Kaapvaal craton. *Earth Planet. Sci. Lett.* **120,** 13–29.

Irvine G. J., Kopylova M. G., Carlson R. W., Pearson D. G., Shirey S. B., and Kjarsgaard B. A. (1999) Age of the lithospheric mantle beneath and around the Slave craton: A Rhenium-Osmium isotopic study of peridotite xenoliths from the Jericho and Somerset Island kimberlites. Ninth Ann. V. M. Goldschmidt Conference. *LPI Contribution,* **971,** 134–135.

Jones R. A. (1987) Strontium and neodymium isotopic and rare earth element evidence for the genesis of megacrysts in kimberlites of southern Africa. In *Mantle Xenoliths* (ed. P. H. Nixon), pp. 711–724. John Wiley & Sons, Chichester.

Kramers J. D. (1977) Lead and strontium isotopes in Cretaceous kimberlites and mantle-derived xenoliths from southern Africa. *Earth Planet. Sci. Lett.* **34,** 419–431.

Kramers J. D., Roddick J. C. M., and Dawson J. B. (1983) Trace element and isotope studies on veined, metasomatic and "MARID" xenoliths from Bultfontein, South Africa. *Earth Planet. Sci. Lett.* **65,** 90–106.

Manhès G., Allègre C. J., Dupré B., and Hamelin B. (1980) Lead isotope study of basic-ultrabasic layered complexes: Speculations about the age of the earth and primitive mantle characteristics. *Earth Planet. Sci. Lett.* **47,** 370–382.

Macdougall J. D. and Haggerty S. E. (1999) Ultradeep xenoliths from African kimberlites: Sr and Nd isotopic compositions suggest complex history. *Earth Planet. Sci. Lett.* **170,** 73–82.

McCulloch M. T., Jaques A. L., Nelson D. R., and Lewis J. D. (1983) Nd and Sr isotopes in kimberlites and lamproites from Western Australia: An enriched mantle origin. *Nature* **302,** 400–403.

McDonough W. F. (1990) Constraints on the composition of the continental lithospheric mantle. *Earth Planet. Sci. Lett.* **101,** 1–18.

McDonough W. F. and Sun S. S. (1995) The composition of the earth. *Chem. Geol.* **120,** 223–253.

Menzies M. A. (1990) Archean, Proterozoic, and Phanerozoic lithospheres. In *Continental Mantle* (ed. M. A. Menzies), pp. 67–86. Oxford University Press, Oxford.

Menzies M. A. and Murthy R. (1980) Enriched mantle: Nd and Sr isotopes in diopsides from kimberlite nodules. *Nature* **283,** 634–636.

Menzies M. A., Rogers N., Tindle A., and Hawkesworth C. J. (1987) Metasomatic and enrichment processes in lithospheric peridotites, an effect of asthenosphere-lithosphere interaction. In *Mantle Metasomatism* (eds. M. Menzies and C. J. Hawkesworth), pp. 313–361. Academic Press, London.

Mitchell R. H. (1995) *Kimberlites, Orangeites, and Related Rocks*. Plenum Press, New York.

Nixon P. H. (1987) Kimberlitic xenoliths and their cratonic setting. In *Mantle Xenoliths* (ed. P. H. Nixon), pp. 215–239. John Wiley, Chichester.

Pearson D. G. (1999) The age of continental roots. *Lithos* **48,** 171–194.

Pearson D. G., Carlson R. W., Shirey S. B., Boyd F. R., and Nixon P. H. (1995a) Stabilisation of Archean lithospheric mantle: A Re-Os isotope study of peridotite xenoliths from the Kaapvaal craton. *Earth Planet. Sci. Lett.* **134,** 341–357.

Pearson D. G., Shirey S. B., Carlson R. W., Boyd F. R., Pokhilenko N. P., and Shimizu N. (1995b) Re-Os, Sm-Nd, and Rb-Sr isotope evidence for thick Archean lithospheric mantle beneath the Siberian craton modified by multistage metasomatism. *Geochim. Cosmochim. Acta* **59**, 959–977.

Pell J. (1993) New kimberlite discoveries on Somerset Island. In *Exploration Overview 1993*, p. 47. NWT Geology Division, Department of Indian and Northern Affairs, Yellowknife.

Richardson S. H., Erlank A. J., and Hart S. R. (1985) Kimberlite-borne garnet peridotite xenoliths from old enriched subcontinental mantle. *Earth Planet. Sci. Lett.* **75,** 116–128.

Ringwood A. E., Kesson S. E., Hibberson W., and Ware N. (1992) Origin of kimberlites and related magmas. *Earth Planet. Sci. Lett.* **113,** 521–538.

Schmidberger S. S. and Francis D. (1999) Nature of the mantle roots beneath the North American craton: Mantle xenolith evidence from Somerset Island kimberlites. *Lithos* **48,** 195–216.

Schmidberger S. S. and Francis D. (2001) Constraints on the trace element composition of the Archean mantle root beneath Somerset Island, Arctic Canada. *J. Petrol.* **42,** 1095–1117.

Smith C. B. (1983) Pb, Sr and Nd isotopic evidence for sources of southern African Cretaceous kimberlites. *Nature.* **304,** 51–54.

Smith C. B., Allsopp H. L., Garvie O. G., Kramers J. D., Jackson

P. F. S., and Clement C. R. (1989) Note on the U-Pb perovskite method for dating kimberlites: Examples from the Wesselton and DeBeers mines, South Africa, and Somerset Island, Canada. *Chem. Geol. (Isot. Sect.)* **79,** 137–145.

Stacey J. S. and Kramers J. D. (1975) Approximation of terrestrial lead isotope evolution by a two-stage model. *Earth Planet. Sci. Lett.* **26,** 207–223.

Steward W. D. (1987) Late Proterozoic to Early Tertiary stratigraphy of Somerset Island and northern Boothia Peninsula, District of Franklin. *Geological Survey of Canada Paper* **83–26,** 78.

Trettin H. P. (1991) Geology of Canada: Summary and remaining problems. In *Geology of the Innuitian orogen and Arctic platform of Canada and Greenland* (ed. H. P. Trettin), pp. 547–553. Geological Survey of Canada.

Walker R. J., Carlson R. W., Shirey S. B., and Boyd F. R. (1989) Os, Sr, Nd, and Pb isotope systematics of southern African peridotite xenoliths: Implications for the chemical evolution of subcontinental mantle. *Geochim. Cosmochim. Acta* **53,** 1583–1595.

Woolley A. R. and Kempe D. R. C. (1989) Carbonatites nomenclature, average chemical compositions, and elemental distribution. In *Carbonatites; Genesis and Evolution* (ed. K. Bell), pp. 1-14. Unwin Hyman, London.

Zindler A. and Hart S.R. (1986) Chemical Geodynamics. *Ann. Rev. Earth Planet. Sci.* **14,** 493–571.